Available online at www.sciencedirect.com
ScienceDirect
Geochimica et Cosmochimica Acta 70 (2006) 4862–4873
Geochimica
www.elsevier.com/locate/gca

Enthalpies and entropies of proton and cadmium adsorption onto *Bacillus subtilis* bacterial cells from calorimetric measurements

Drew Gorman-Lewis [a,*], Jeremy B. Fein [a], Mark P. Jensen [b]

[a] *Civil Engineering/Geological Sciences, University of Notre Dame, 156 Fitzpatrick Hall, Notre Dame, IN 46616, USA*
[b] *Chemistry Division, Argonne National Lab, Argonne, IL 60439, USA*

Received 26 October 2005; accepted in revised form 20 July 2006

Abstract

We used titration calorimetry to measure the bulk heats of proton and Cd adsorption onto a common Gram positive soil bacterium *Bacillus subtilis* at 25.0 °C. Using the 4-site non-electrostatic model of Fein et al. [Fein, J.B., Boily, J.-F., Yee, N., Gorman-Lewis, D., Turner, B.F., 2005. Potentiometric titrations of *Bacillus subtilis* cells to low pH and a comparison of modeling approaches. *Geochim. Cosmochim. Acta* **69** (5), 1123–1132.] to describe the bacterial surface reactivity to protons, our bulk enthalpy measurements can be used to determine the following site-specific enthalpies of proton adsorption for Sites 1–4, respectively: -3.5 ± 0.2, -4.2 ± 0.2, -15.4 ± 0.9, and -35 ± 2 kJ/mol, and these values yield the following third law entropies of proton adsorption onto Sites 1–4, respectively: $+51 \pm 4$, $+78 \pm 4$, $+79 \pm 5$, and $+60 \pm 20$ J/mol K. An alternative data analysis using a 2-site Langmuir–Freundlich model to describe proton binding to the bacterial surface (Fein et al., 2005) resulted in the following site-specific enthalpies of proton adsorption for Sites 1 and 2, respectively: -3.6 ± 0.2 and -35.1 ± 0.3 kJ/mol. The thermodynamic values for Sites 1–3 for the non-electrostatic model and Site 1 of the Langmuir–Freundlich model of proton adsorption onto the bacterial surface are similar to those associated with multifunctional organic acid anions, such as citrate, suggesting that the protonation state of a bacterial surface site can influence the energetics of protonation of neighboring sites. Our bulk Cd enthalpy data, interpreted using the 2-site non-electrostatic Cd adsorption model of Borrok et al. [Borrok, D., Fein, J.B., Tischler, M., O'Loughlin, E., Meyer, H., Liss, M., Kemner, K.M., 2004b. The effect of acidic solutions and growth conditions on the adsorptive properties of bacterial surfaces. *Chem. Geol.* **209** (1–2), 107–119.] to account for Cd adsorption onto *B. subtilis*, yield the following site-specific enthalpies of Cd adsorption onto bacterial surface Sites 2 and 3, respectively: -0.2 ± 0.4 and $+14.4 \pm 0.9$ kJ/mol, and the following third law entropies of Cd adsorption onto Sites 2 and 3, respectively: $+57 \pm 4$ and $+128 \pm 5$ J/mol K. The calculated enthalpies of Cd adsorption are typical of those associated with Cd complexation with anionic oxygen ligands, and the entropies are indicative of inner sphere complexation by multiple ligands. The experimental approach described in this study not only yields constraints on the molecular-scale mechanisms involved in proton and Cd adsorption reactions, but also provides new thermodynamic data that enable quantitative estimates of the temperature dependence of proton and Cd adsorption reactions.

1. Introduction

The adsorption of metals onto bacterial surfaces can control the mobility and speciation of metals in a wide range of environments. Despite recent advances made by bulk adsorption measurements and spectroscopic investigations, we still lack a full understanding of bacterial cell wall reactivity and the mechanisms that control cell wall adsorption. Calorimetric measurements of proton and metal adsorption onto bacterial cell walls not only can provide rigorous constraints on bulk proton and metal adsorption, but interpretation of these data can give site-specific enthalpies and entropies of proton and metal adsorption onto the bacterial surface functional groups, yielding information on coordination environment, as well as the temperature dependence of the adsorption reactions.

* Corresponding author.
E-mail address: gorman-lewis@anl.gov (D. Gorman-Lewis).

0016-7037/$ - see front matter © 2006 Elsevier Inc. All rights reserved.
doi:10.1016/j.gca.2006.07.022

A range of experimental techniques has been used to study bacterial surface adsorption reactions. Potentiometric titrations measure proton adsorption, and can be used to determine acidity constants and site concentrations of the important functional groups on the bacterial cell wall (Plette et al., 1995; Fein et al., 1997; Daughney and Fein, 1998; Cox et al., 1999; Haas et al., 2001; Sokolov et al., 2001; Yee and Fein, 2001; Martinez et al., 2002; Ngwenya et al., 2003; Yee et al., 2004; Fein et al., 2005). Bulk metal adsorption experiments measure the affinity for metals to adsorb onto the bacterial surface, and surface complexation modeling of these results yields thermodynamic stability constants for the important bacterial surface complexes (Fein et al., 1997; Fowle and Fein, 1999; Fowle et al., 2000; Haas et al., 2001; Daughney et al., 2002; Ngwenya et al., 2003; Borrok et al., 2004a; Chatellier and Fortin, 2004; Gorman-Lewis et al., 2005). Although potentiometric titrations and bulk adsorption experiments provide rigorous constraints on the total reactivity of the cell wall, they do not provide complete or detailed information on the binding environments, and hence the derived thermodynamic property values are dependent on the binding models chosen to represent the bacterial surface reactivity. Spectroscopic data provide more direct evidence of the metal coordination environment than do bulk adsorption measurements, and X-ray absorption spectroscopy (XAS) has been used to constrain the binding environment of metal cations on cell wall functional groups (Hennig et al., 2001; Kelly et al., 2002; Panak et al., 2002; Boyanov et al., 2003). However, due to the complexity of the cell wall binding environments, and due to the fact that XAS yields an averaged binding environment, the experimental results from XAS can be complex and difficult to interpret. For example, although XAS has been used successfully to demonstrate the importance of carboxyl and phosphoryl binding sites for U and Cd on the bacterial cell wall of *Bacillus subtilis*, significant uncertainties exist regarding the metal: ligand stoichiometry involved in binding (Kelly et al., 2002; Boyanov et al., 2003). Clearly, complementary lines of evidence are needed to constrain mechanisms of proton and metal adsorption onto bacterial cell walls.

Calorimetric measurements of proton and metal binding onto bacterial surfaces, interpreted using a surface complexation modeling approach, can be used to infer site-specific enthalpies and entropies of adsorption. Weppen and Hornburg (1995) used flow calorimetry and bulk adsorption experiments to compare the metal sequestration capability of cell wall suspensions harvested from a range of bacterial cells. Their measured bulk enthalpies of metal adsorption (for Cd, Cu, Zn, Pb, Mg, Ca, Sr, Ba) were all modestly endothermic (+3 to +18 kJ/mol with a value of +10.4 kJ/mol for Cd), and in the expected range for divalent cations coordinated with anionic oxygen ligands. However, Weppen and Hornburg (1995) did not correct for the heat associated with protonation reactions, and used a bulk partitioning approach instead of a site-specific surface complexation model to quantify metal adsorption. In this study, we use calorimetric data, in conjunction with surface complexation models of the bacterial cell wall, to produce site-specific enthalpies of proton and Cd adsorption onto the cell wall of *B. subtilis*, a common Gram-positive aerobic soil bacterial species. Our calorimetric measurements, made using actual bacteria, allow the determination of site-specific metal adsorption enthalpies. In addition, the heats of proton adsorption, which are needed to correct the data from the metal adsorption titrations, also may be used to constrain the nature and reactivity of cell wall binding sites. The heat of protonation data were interpreted using both a site-specific model and a generalized surface complexation (Langmuir–Freundlich) model. The thermochemical pictures that emerge from both models are similar. These data provide information regarding the likely structure of the functional groups on the bacterial surface, the usefulness of simple organic acids as proxies for these sites, and the temperature dependence of the acidity constants.

2. Experimental procedures

2.1. Cell preparation

Bacillus subtilis cells (supplied originally by T.J. Beveridge, University of Guelph) were cultured and prepared following the procedures outlined previously (Fein et al., 1997; Fowle et al., 2000) except the acid wash step in the cell preparation was not conducted in order to avoid possible acid damage to the cell walls (Borrok et al., 2004b). Cells were maintained on agar plates consisting of trypticase soy agar with 0.5% yeast extract added. Cells for the adsorption experiments were grown by first inoculating a test-tube containing 3 mL of trypticase soy broth and 0.5% yeast extract, and incubating it for 24 h at 32 °C. The 3 mL bacterial suspension was then transferred to a 1 L volume of broth, also with 0.5% yeast extract, and allowed to grow for another 24 h on an incubator shaker table at 32 °C. Cells were pelleted by centrifugation at 1600*g* for 15 min, and rinsed seven times with 0.1 M $NaClO_4$. The bacteria were then pelleted by centrifugation at 5000*g* for 60 min to remove excess water so suspensions of known bacterial concentration could be created. Previous studies have shown this bacterial preparation method, including the high speed centrifugation step to pellet the bacteria, does not cause cell lysis and that cells remain intact for up to 72 h (Lee and Fein, 2000). The ratio of the wet weight of the pelleted bacteria to dry weight is 5.1:1 (Borrok et al., 2004b).

2.2. Bulk adsorption experiments

The calorimetric measurements made in this study yield the heat of adsorption that occurs upon titration of an adsorbate (either $HClO_4$ or $Cd(ClO_4)_2$ solutions) into a bacterial suspension. These data can be most simply interpreted if the experiments are conducted under conditions

where virtually all of the adsorbate added to the system binds to the surface of interest, eliminating contributions to the measured total heat from other sources such as aqueous complexation reactions involving the added metal ions and organic exudates from the bacteria. In order to quantify the extent of Cd adsorption onto the bacterial cells under all of the conditions present during the calorimetry experiments, we conducted two types of preliminary adsorption experiments: (1) bulk adsorption measurements, conducted as a function of Cd concentration and pH (from pH 2 to 9 using small amounts of concentrated HNO_3 and NaOH to adjust pH) to directly mirror the Cd calorimetry experimental conditions; and (2) Cd adsorption kinetics experiments to determine the time to reach adsorption equilibrium under the experimental conditions, and thus and the speed at which the calorimetric titrations could proceed. We used a bacterial concentration of approximately 80 g wet mass/L in the calorimetry experiments in order to obtain a measurable response, so this same concentration was used in each of the adsorption control experiments. We measured the extent of Cd adsorption as a function of pH, suspending the bacteria in a solution containing 5.3×10^{-4} M $Cd(ClO_4)_2$ with 0.1 M $NaClO_4$ to buffer ionic strength, following a similar procedure outlined by Borrok et al. (2004b). Concentration dependent adsorption experiments were performed by suspending the bacteria in 0.1 M $NaClO_4$ adjusted to pH 6.18 and adding $Cd(ClO_4)_2$ to obtain total Cd concentrations ranging from 0.04 to 0.53 mM (the range of Cd concentrations encountered during the calorimetric titrations). Adsorption kinetics experiments were performed with the bacterial suspension containing a Cd concentration of 5.3×10^{-4} M adjusted to pH 6.30. Samples were extracted at 30 s time intervals, similar to the procedure outlined in Fowle et al. (2000). Samples from each control experiment were analyzed for aqueous Cd by inductively coupled plasma optical emission spectroscopy with matrix-matched standards. The analytical uncertainty was ±3.5% with a detection limit of 5 ppb.

The adsorption kinetics experiments demonstrated that Cd adsorption onto the bacterial surfaces was complete within 30 s after introduction of the Cd to the bacterial suspension. We also observed 100% adsorption of Cd within the experimental uncertainty (±3.5%) at or above pH 5.3 and at all Cd concentrations studied. This ensures that the heats measured by titration calorimetry under these conditions are a result of Cd-bacterial adsorption reactions and not simple aqueous complexation reactions occurring between the Cd and bacterial exudates. It is also consistent with previous studies that found *B. subtilis* bacterial exudates had no measurable proton binding capacity (Wightman et al., 2001); consequently, the ability of these exudates to complex metals is likely to be small. In addition, because these control experiments were designed to mimic conditions as close as possible to those employed in the calorimetry experiments, we conclude that all of the Cd that is added to the bacterial suspensions during each step of the calorimetric titration adsorbs onto the bacteria, and that the adsorption reaction goes to completion rapidly (in less than 30 s).

2.3. Titration calorimetry

The calorimetric titrations were conducted with an isothermal titration microcalorimeter (Calorimetry Sciences Corporation, Model ITC 4200), which measures the heat flow between a reaction cell and a reference cell. The calorimeter's response to the heat flow was calibrated by electrical heating, a procedure that we have previously verified by checking the reported protonation heat of tris-hydroxymethylaminomethane (TRIS/THAM) at 25 °C (Grenthe et al., 1970). Initially, both cells were filled with identical solutions (in this case, a bacterial suspension containing 0.1 M $NaClO_4$ to buffer ionic strength) and placed in the calorimeter bath. The bacterial suspension in the reaction cell was stirred at 300 rpm with a motor driven stainless steel paddle. After thermal equilibrium with the water bath (24.995 ± 0.005 °C) and a sufficiently constant background heat flow between the reaction and reference cells were achieved, a predetermined number of individual titrant doses were delivered into the reaction cell via a needle from 100 to 250 μL syringe driven by a computer-controlled motor. Each titrant addition was followed by a period between 300 and 600 s, depending on the titrant, where the heat flow between the reaction and reference cells, due to addition and reaction of each dose, was measured continuously.

Two types of calorimetric measurements were conducted: (1) protonation experiments in which acid was titrated into the reaction cell to sequentially protonate bacterial cell wall functional groups; and (2) Cd adsorption experiments in which a Cd-bearing solution was titrated into the reaction cell at a nearly constant pH. All the titrations were performed with 900 μL of 80 g/L bacterial suspension in 0.1 M $NaClO_4$. The pH of the suspension was adjusted to the appropriate pH by the addition of $HClO_4$ or carbonate-free NaOH prior to the titration. The titrant composition was either 0.170 M $HClO_4$ for the protonation titrations or 5.3×10^{-3} M $Cd(ClO_4)_2$ in 0.1 M $NaClO_4$, adjusted to match the pH of the bacterial suspension.

We gathered the protonation data under two different initial experimental conditions where the initial pH of the bacterial suspension was adjusted between pH 6.4 and 7.0 (low pH) or to pH 10.0 (high pH). A single titration from pH 10 to 2.5 that would measure the protonation heats for all four sites could not be conducted due to limitations on the number of possible titrant additions by the calorimeter. A wider pH range could have been covered using a more concentrated acid as the titrant, but this would have caused the magnitude of the heats generated by protonation of the bacterial surface to be well outside the ideal range of heats for the calorimeter. For the high pH titration, we used sequential 1 μL additions of 0.170 M $HClO_4$ and obtained a final pH of ca. 6. In order to optimize the calorimetric

response for the low pH titrations, in which the heats generated by protonation of the bacterial suspension were smaller than those from the high pH titrations, we used 20 sequential 5 μL additions of 0.170 M $HClO_4$, obtaining a final pH between 2.50 and 2.61, depending on the initial pH of the solution. Low pH titrations were performed in triplicate and high pH titrations were performed in duplicate. Additional experiments measuring the background heats that were not caused by proton adsorption (i.e., the heat of dilution and other heats associated with the experimental apparatus such as the heat of titrant injection), were performed by titrating 0.170 M $HClO_4$ into a bacteria-free solution of 0.1 M $NaClO_4$ adjusted to pH 6.93. It was unnecessary to perform similar blank titrations at higher pH since these background heats are independent of pH under the experimental conditions.

For the Cd adsorption titrations, the reaction and reference cells were filled with 900 μL of an 80 g/L bacterial suspension in 0.1 M $NaClO_4$ adjusted to pH values of 6.01 or 5.33. The titrant used was a 5.3×10^{-3} M $Cd(ClO_4)_2$ solution in 0.1 M $NaClO_4$ adjusted to match the pH of the bacterial suspension. In each experiment, sequential 8 μL doses of titrant were added to the reaction cell, and the experiments were performed in duplicate at each pH. Drift in the solution pH over the course of the experiment was minimal as indicated by the final pH value in the reference cell, which was 5.95 and 5.34, respectively, for experiments that started at pH 6.01 and 5.33; therefore, buffering the pH of the titrations was not necessary. We measured the background heats in the Cd titration experiments (i.e., the heats that were not caused by Cd adsorption), by titrating the same Cd-bearing solution into a bacteria-free solution of 0.1 M $NaClO_4$ adjusted to pH 6.04 or 5.32.

In order to obtain the heat associated with reactions on the bacterial cell wall after the xth addition of titrant, Q_x^{corr}, we subtracted the background heat that was measured for the addition of an identical amount of titrant to a bacteria-free system, Q_x^{bkg}, from the experimentally measured heat associated with a given titrant addition, Q_x^{exp},

$$Q_x^{corr} = Q_x^{exp} - Q_x^{bkg}. \quad (1)$$

This background correction is pH independent and accounts for the heat of dilution and for other heats intrinsic to the titration process. In addition to the heat of dilution when the solution exceeds pH ~8.5, it is also necessary to correct for the heat of hydroxide neutralization associated with the reaction $H^+ + OH^- \rightarrow H_2O$ that occurs on the addition of acid or liberation of protons from the bacterial surface by metal binding. The enthalpy for this reaction in 0.1 M $NaClO_4$ was estimated to be -56.48 ± 0.09 kJ/mol by interpolation of the heats of NaOH neutralization reported for HCl and $HClO_4$ in solutions with ionic strengths between 0.005 and 3 M (Hale et al., 1963; Vanderzee and Swanson, 1963; Martell et al., 1998). In our work, correction for the heat of hydroxide neutralization was only necessary for the high pH, above pH 8.6, protonation experiments. In those cases, the heat of hydroxide neutralization with each addition of acid was calculated from the enthalpy of neutralization, the initial solution pH, the total amount of acid added, the concentration of protolyzable bacterial surface sites, and the pK_a values of those sites and was included in the Q_x^{bkg} term in Eq. (1). A previous study has shown that organics exuded by *B. subtilis* have no proton buffering capacity and consequently do not need to be accounted for in the correction term (Wightman et al., 2001). By convention, the calorimeter software assigns positive values to measured exothermic heats and negative values to endothermic heats.

The concentration of each species in the suspension was calculated for each point in the titration using the program PSEQUAD (Zekany and Nagypal, 1985) from the known initial pH and the total concentrations of bacteria, acid and metal in the reaction vessel. Measurements of pH are not possible during the titration. Therefore, the pH values, we report for the individual titration points also come from the speciation calculations. Site-specific equilibrium constants for binding at each site on the bacteria surface were taken from the 4-site speciation model of Fein et al. (2005) for the protonation reactions and from Borrok et al. (2004b) for the Cd adsorption reactions. We also tested the dependence of the calculated thermodynamic parameters on the titration model used by conducting similar speciation calculations for the bacterial surface using FITEQL (Herbelin and Westall, 1994) and invoking the Langmuir–Freundlich protonation model of Fein et al. (2005). The solution volume and the concentrations calculated by PSEQUAD or FITEQL for each point of the titration were then used as independent variables to derive the enthalpies of reaction from the calorimetric data as least-squares fitted parameters with the program Origin 5.0 (Microcal), as described below. The uncertainties in the thermodynamic parameters are given at the 95% (2σ) confidence level and are calculated for the enthalpies either as the standard error in the average, or from the inverse of the covariance matrix of a given fit.

3. Results and discussion

3.1. Protonation reactions

The thin curve in Fig. 1 depicts the raw calorimetry data from a typical low pH experimental run, illustrating the heat evolved for each addition of 5 μL of 0.17 M $HClO_4$ to the bacterial suspension. The heavy curve represents the background heat (scaled up by a factor of 10) generated from the control titrations conducted under similar conditions in the absence of bacteria. The initial pH of the system was 6.87, and the pH after equilibration of the final addition was 2.61. Calculated pH values at the end of the titration from the two models used to describe proton adsorption, explained below, were 2.60 and 2.57 for the 4-site non-electrostatic and the 2-site Langmuir–Freundlich continuum models of Fein et al. (2005), respectively. The corrected heats for the protonation titration ($Q_x^{prot,corr}$) are

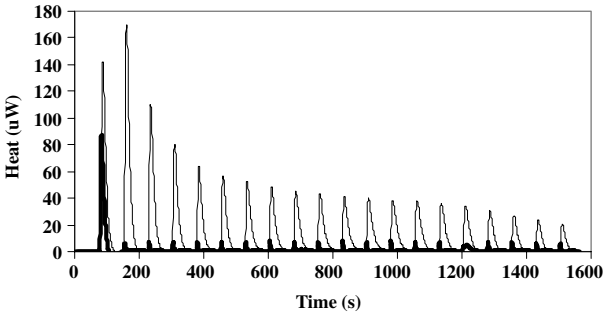

Fig. 1. Raw data from a typical low pH proton adsorption titration (–) with the measured heat of dilution (scaled up by a factor of 10) for each corresponding addition of acid (—).

the experimental heats (the integrated area under the thin curve) minus the background heats. Figs. 2 and 3 report the corrected heats generated from protonation of the low and high pH bacterial suspension, respectively.

The heat associated with the first addition of titrant is not considered in our data analysis. Over the several hour period required for the reaction vessel to reach thermal equilibrium with the water bath, titrant will diffuse into the reaction vessel unless the titrant and the titrant are separated by a small air gap. The effect on the measured heat

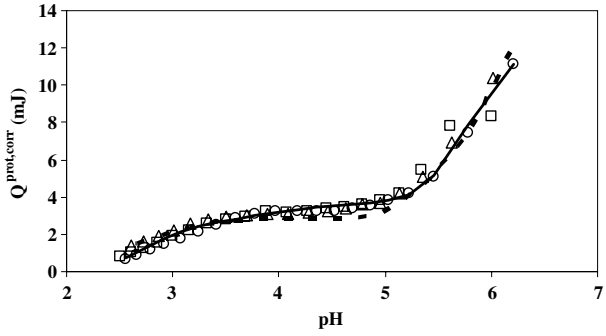

Fig. 2. Corrected heat evolved from three low pH proton adsorption titrations of 80 g/L *B. subtilis*, with the solid curve and the dashed curve representing the fit of the 4-site non-electrostatic or the Langmuir–Freundlich model to Eq. (3), respectively. Positive Q represents exothermic heats. pH Values are from the speciation calculations.

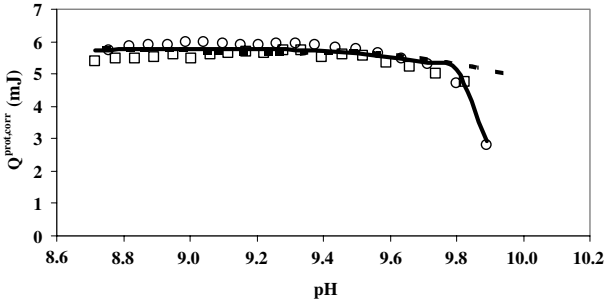

Fig. 3. Corrected heat evolved from two high pH proton adsorption titrations of 80 g/L *B. subtilis*, with the solid curve and the dashed curve representing the fit of the 4-site non-electrostatic or the Langmuir–Freundlich model to Eq. (3), respectively. Positive Q represents exothermic heats. pH Values are from the speciation calculations.

of the first addition can be neglected if the volume of the diffused titrant or the air gap are small relative to the volume of the titrant addition. That approximation does not hold for the small volumes of titrant added in our experiments. Instead, the titrant is allowed to diffuse into the bacterial suspensions during the initial equilibration period. Because of this diffusion, one cannot know exactly how much titrant reacts during the first addition, but one does know that all of the titrant intended to be added in the first addition (the sum of the diffused titrant and the titrant actually added), is in the vessel at the end of the first addition. Knowing this, the solution speciation can be calculated at that point and the more rapid sequential additions can continue as planned with diffusion playing a negligible role in the measured heats of the subsequent additions.

The calorimetry measurements demonstrate that the protonation reactions at the bacterial surface are distinctly exothermic and that significant proton adsorption occurs continuously over the entire pH range studied. Wightman et al. (2001) found *B. subtilis* exudates had no measurable proton binding capacity. Consequently, protonation of the bacterial exudates is likely an insignificant contributor to the measured heat, and is not considered in the analysis. Further interpretation of the bulk enthalpy data requires the application of a surface complexation model to the bacterial surface to assign proton adsorption to specific functional groups. The resulting site-specific thermodynamic parameters can be used to constrain specific binding mechanisms involving specific functional groups on the bacterial surface. However, the distributions of the total heat over the specific sites will be directly dependent on the model chosen to describe the acidity constants of the cell wall functional groups. Nevertheless, considering the raw calorimetric data, the site-specific enthalpies derived from the measured calorimetric data will be exothermic regardless of the protonation model selected.

While the various models describing proton binding on the bacterial surface may differ in the number of proton-active sites and the ease of protonation at those sites, the protonation of a given proton-active functional group can generally be expressed as

$$\mathrm{R{-}L}_i^- + \mathrm{H}^+ \leftrightarrow \mathrm{R{-}L}_i\mathrm{H}^\circ \tag{2}$$

where R is a bacterium to which a proton-active functional group type, L_i^-, is attached. Knowing the concentrations of each site, the pH, and the appropriate equilibrium constants, the degree of protonation of each L_i^- group can be calculated for any point along the titration path. For each step of the titration, the protonation enthalpies of each site L_i^-, $\Delta\mathrm{H}_{\mathrm{HL}_i}$, are related to the background corrected heat, $Q_x^{\mathrm{prot,corr}}$, by the equation

$$-Q_x^{\mathrm{prot,corr}} = \sum_i \Delta H_{\mathrm{HL}_i} \Delta n_{\mathrm{HL}_i}^x, \tag{3}$$

where each $\Delta n_{\mathrm{HL}_i}^x$ is the change in the number of moles of the protonated species HL_i caused by the xth addition of titrant. Because the calculated $\Delta n_{\mathrm{HL}_i}^x$ values are model

dependent, the resulting site-specific enthalpies of protonation are model dependent as well.

To understand the influence of the speciation model on the thermodynamic parameters derived from our calorimetric data, we fit the measured heats to two different equilibrium models of the *B. subtilis* surface, the 4-site non-electrostatic model of Fein et al. (2005) and a 2-site implementation of the Langmuir–Freundlich continuum model (as derived by Koopal et al. (1994)) with model parameters determined for protonation reactions of the *B. subtilis* cell wall by Fein et al. (2005). Both models were capable of reproducing the general form of the free energy and enthalpy of absorption data. However, fits with the 4-site non-electrostatic model always provided more chemically reasonable and statistically better fits to the available data (*vide infra*).

3.2. 4-Site non-electrostatic model data analysis

Fein et al. (2005) have proposed a 4-site non-electrostatic surface complexation model that ascribes proton binding on the surface of *B. subtilis* to four different types of proton-active sites, each with a distinctive pK_a, as described by reaction 2. Using the calorimetric pH titration data in conjunction with the protonation constants from the 4-site non-electrostatic model of Fein et al. (2005) to determine the values of $\Delta n^x_{HL_i}$ in Eq. (3), the site-specific enthalpy of protonation, ΔH_{HL_i} , was calculated for each of the four sites represented by reaction 2. The site-specific protonation enthalpies represent the heat generated by protonation of site L_i^- per mole of protonated site L_i^-. Potentiometric titrations of the bacterial surface constrain the site concentrations and acidity constants for the pertinent protonation reactions, and both the calorimetry data and the prior potentiometric titrations strongly suggest the presence of a cell wall functional group, or groups, with a pK_a (the negative logarithm of the acidity constant of this site), significantly below 4. Fein et al. (2005) modeled this site (Site 1) with a pK_a value of 3.3. The other sites in this model have pK_a values of 4.8, 6.8, and 9.1 for Sites 2–4, respectively.

Comparison of the data from the high and low pH calorimetric titrations between pH 6 and 7 suggests that a small, variable, amount of carbonate contamination, from atmospheric CO_2, was present in the high pH titrations. The construction of the calorimeter provides no convenient way to maintain a CO_2-free atmosphere in the reaction vessel, and high pH solutions can absorb large amounts of CO_2 from the air (the $[CO_3^{2-}]$ in a hypothetical pH 10, 0.1 M ionic strength solution in equilibrium with the atmosphere would be 0.097 M, Martell et al., 1998). From the curvature of the experimentally measured heats between pH 8.8 and 9.9, and the reported enthalpy for CO_3^{2-} protonation, −18.8 kJ/mol (Martell et al., 1998), we estimate the *maximum* concentration of CO_3^{2-} at the start of the high pH titrations to be 0.001 M. While the presence of 0.001 M CO_3^{2-} would cause a +3 kJ/mol (10%) systematic error in the value of ΔH_{HL_4} determined from the high pH titrations, this level of carbonate contamination would have a much larger impact on ΔH_{HL_3}, which normally should be determinable between pH 5.8 and 7.8. This is due to the very large uncertainty in the solution speciation caused by the inaccuracy of the proton balance introduced by failing to quantitatively account for the presence of CO_3^{2-}. Any carbonate contamination will be much smaller in the low pH titrations where the equilibrium total carbonate capacity is much lower and the solution speciation is better constrained by the initial measured pH.

Due to the different effects of CO_2 on the titrations, we split the analysis of the site-specific enthalpies of proton adsorption into two parts for both the 4-site non-electrostatic and the 2-site Langmuir–Freundlich treatments. First, the data from the high pH titrations below pH 8.7 were discarded due to issues of carbonate contamination described above, and the data between pH 8.7 and 9.9 were used to determine ΔH_{HL_4} (or ΔH_{HL_2} for the Langmuir–Freundlich model) from Eq. (3), with the approximations that $\Delta n^x_{HL_i} = 0$ for the other sites and that the influence of CO_3^{2-} on the final protonation enthalpy is small ($\leqslant$10%) in that pH range. The model of Fein et al. (2005) suggests that the uptake of protons on Sites 1–3 is negligible ($\leqslant$1%) when titrating the bacterial suspension from pH 9.9 to pH 8.7, as we do in the high pH titration. Despite these approximations, our high pH titration calorimetry data allow us to constrain the enthalpy of protonation of Site 4 and to determine the influence that the Site 4 protonation enthalpy exerts on the thermochemistry of the protonation reactions occurring below pH 8. The calculated enthalpy of Site 4 from the two high pH experiments is -35 ± 2 kJ/mol, as shown in Fig. 3 and reported in Table 1. However, it should be recognized that this value could be as large as −38 kJ/mol due to the potential systematic error from CO_2 contamination of the high pH solutions.

In the second part of the data analysis, we calculated the site-specific enthalpies of protonation of Sites 1–3 from Eq. (3) using the data from the low pH titrations and the value of ΔH_{HL_4} determined from the high pH titrations. The combination of the 4-site speciation model and Eq. (3) produces an excellent fit (Fig. 2) to the observed corrected heats of surface protonation. The derived enthalpies of

Table 1
Site-specific thermodynamic parameters for the reaction of H^+ and Cd^{2+} with the surface of *B. subtilis* in 0.1 M $NaClO_4$ at 25.0 °C derived from calorimetric titration and the 4-site speciation models of Fein et al. (2005) and Borrok et al. (2004b)

Reaction	log K[a]	$\Delta G°$/kJ/mol	$\Delta H°$/kJ/mol	$\Delta S°$/J/mol K
$H^+ + L_4^- \rightarrow HL_4$	9.1	-51.9 ± 1.1	-35 ± 2	$+60 \pm 20$
$H^+ + L_3^- \rightarrow HL_3$	6.8	-38.8 ± 1.7	-15.4 ± 0.9	$+79 \pm 6$
$H^+ + L_2^- \rightarrow HL_2$	4.8	-27.4 ± 0.6	-4.2 ± 0.2	$+78 \pm 2$
$H^+ + L_1^- \rightarrow HL_1$	3.3	-18.8 ± 1.1	-3.5 ± 0.2	$+51 \pm 4$
$Cd^{2+} + L_2^- \rightarrow CdL_2^+$	3.0	-17.1 ± 1.1	-0.2 ± 0.4	$+57 \pm 4$
$Cd^{2+} + L_3^- \rightarrow CdL_3^+$	4.2	-23.7 ± 1.1	$+14.4 \pm 0.9$	$+128 \pm 5$

[a] $K = [R - L_i^- - M][M]^{-1}[R - L_i^-]^{-1}$, where $M = H^+$ or Cd^{2+}.

proton adsorption are -3.5 ± 0.2, -4.2 ± 0.2, and -15.4 ± 0.9 kJ/mol for Sites 1–3, respectively. Despite the much larger uncertainty associated with the enthalpy of proton absorption at Site 4, the pK_a of Site 4 is sufficiently different from the pK_a values of the other sites that the enthalpy of Site 4 does not significantly influence the other enthalpies. The exact value used for ΔH_{HL_4} can be varied over a wide range (between 0 and -50 kJ/mol) without changing the protonation enthalpies derived for Sites 1 and 2, and with minimal impact (<0.5 kJ/mol, or 1σ) on the protonation enthalpy of Site 3. Under the four site model, protonation reactions of Site 4 are also unimportant in the pH ranges used for the Cd titrations.

Site-specific standard-state entropies of protonation can be calculated from known values of the standard-state Gibbs free energy and enthalpy of protonation

$$\Delta G^{\circ}(HL_i) = \Delta H^{\circ}(HL_i) - T\Delta S^{\circ}(HL_i), \quad (4)$$

where T is absolute temperature, $\Delta G^{\circ}(HL_i)$ is the change in the standard-state Gibbs free energy, $\Delta H^{\circ}(HL_i)$ is the change in the standard-state enthalpy, and $\Delta S^{\circ}(HL_i)$ is the change in the standard-state entropy from the protonation of site L_i^- as described by Eq. (2). The determination of the site-specific enthalpy values required for these calculations is described above; the standard-state Gibbs free energy value for each site is determined directly from the acidity constant for each type of functional group on the bacterial surface through the mass action equation

$$\log K_{HL_i} = \frac{\Delta G^{\circ}(HL_i)}{2.303RT}, \quad (5)$$

where K_{HL_i} is the acid *dissociation* constant of protonated Site HL_i, and R is the universal gas constant. The calculated entropies of proton adsorption, with propagated uncertainties, are $+51 \pm 4$, $+78 \pm 4$, $+79 \pm 5$, and $+60 \pm 20$ J/mol K for Sites 1–4, respectively.

3.3. Langmuir–Freundlich model data analysis

Each of the types of acidic sites previously identified on the surface of *B. subtilis* is comprised of many similar, individual functional groups (e.g., R–COO^- moieties), with similar pK_a values, which interact with each other and with other components of the cell surface. It is often assumed that these interactions are important because the environment experienced by the first protons to go onto a particular type of site (L_i^-) could be significantly different from the environment encountered by the last protons to bind to that type of site. If this were true the actual enthalpy and entropy of the first proton bound to a particular L_i^- would likely be somewhat different from that of the last proton bound to that type of site. For this reason, we also performed an alternative data analysis using a Langmuir–Freundlich model to describe proton binding to the bacterial surface. The Langmuir–Freundlich model is a continuum surface complexation model that distributes proton binding over multiple sites (Koopal et al., 1994), and may be described by the following equation for the expression for the total concentration of deprotonated sites on the bacterial surface

$$\sum[R - L_i^-] = \sum_1^i \frac{[R - L_iH]_{tot}}{1 + (a_{H+} \cdot \beta_i)^m}, \quad (6)$$

where the expression is summed for each of the n functional groups on the cell wall with a protonation constant equal to β_i, R is a bacterium to which a proton-active functional group type is bound, $[R - L_iH]_{tot}$ is the total molar concentration of the nth functional group, and the constant m controls the width of the β_i distribution function. For the Fein et al. (2005) model of *B. subtilis* cells, m has a value of 0.5. Using this model Fein et al. (2005) were equally able to fit the same potentiometric titration data used to constrain their 4-site non-electrostatic model to a 2-site Langmuir–Freundlich model, with apparent pK_a($\log \beta_i$) values of 4.2 (Site 1) and 9.5 (Site 2).

We used the same calorimetric pH titration data, in conjunction with these apparent pK_a values and the Langmuir–Freundlich model, to calculate the site-specific enthalpy of protonation for the two sites represented in Eq. (6). Using the same approach described above for the 4-site model, we used FITEQL to calculate a new set of $\Delta n^x_{HL_i}$ values for each titrant addition using the 2-site Langmuir–Freundlich model. We then used these new $\Delta n^x_{HL_i}$ values as independent variables in Eq. (3) to derive ΔH_{HL_i} values for Langmuir–Freundlich Sites 1 and 2 from the values of $Q_x^{prot,corr}$ for the corresponding titrant addition. The derived enthalpies of proton adsorption are -3.6 ± 0.2 for Site 1 (apparent p$K_a = 4.2$), and -35.1 ± 0.3 kJ/mol for Site 2 (apparent p$K_a = 9.5$). The agreement of these enthalpies with those derived for the sites with similar pK_a's under the 4-site non-electrostatic model (Table 1) is striking. It suggests that the constraints on the speciation imposed by the independent potentiometric titrations cause the enthalpies derived from the corresponding calorimetric data to be more dependent on the protonation constant of the site than the model used to arrive at that constant. In this case, it also seems that the actual enthalpies of protonating a particular site do not change significantly as the proton loading of the site changes as illustrated by the very different proton loading behaviors of the two models that produced very similar enthalpies of protonation.

Despite these general similarities of the protonation enthalpies derived from the two different surface models, the 4-site non-electrostatic model provides a significantly better fit. While Figs. 2 and 3 illustrate that the Langmuir–Freundlich model provides a reasonable fit to the calorimetric data, the superiority of the 4-site model in reproducing the data is particularly apparent between pH 4 and 5 (Fig. 2) above pH 9.7 (Fig. 3). Statistically speaking, the 4-site non-electrostatic model provides a significantly better fit, as measured by the reduced χ^2, which is three times smaller than that of the Langmuir–Freundlich 2-site model. Although, the two site Langmuir–Freundlich

model adequately represented the potentiometric protonation data in previous work (Fein et al., 2005), it is less able to represent the calorimetric data. Consequently, the remaining interpretation and analysis focuses on the 4-site model non-electrostatic model.

3.4. Interpretation of the proton adsorption reactions under the 4-site model

Previous workers have been able to use the characteristic thermodynamic parameters of various ligand groups to identify and quantify acidic sites in other large, complex molecules such as proteins or humic acids (Jespersen and Jordan, 1970; Perdue, 1978). Considering the 4-site model of the *B. subtilis* surface, spectroscopic evidence suggests that Site 2 is likely composed of carboxylate functionalities, while Sites 1 and 3 are likely organo-phosphonic acid groups with different degrees of protonation (Kelly et al., 2002; Boyanov et al., 2003). The protonation of simple monofunctional carboxylic acids, e.g., acetate, and the first protonation of simple organic phosphates ($R–OPO_3^{2-}$) are characterized by endothermic to thermoneutral protonation enthalpies and protonation entropies on the order of +80 to +120 J/mol K (Christensen et al., 1967; Christensen et al., 1976; Martell et al., 1998). This is not in good agreement with our site-specific thermodynamic parameters (exothermic enthalpies and entropies <80 J/mol K). However, while the entropies for the addition of the first proton to multifunctional carboxylic acids, such as citrate or malonate, usually are similar to those of the monofunctional acids, the addition of subsequent protons to other acid groups within the molecule is marked by sequentially smaller, though still positive, protonation entropies (Christensen et al., 1967; Christensen et al., 1976; Martell et al., 1998) because of statistical and physical effects (King, 1965; Nancollas, 1966). This trend in the entropies for successive protonations is also observed for other multifunctional acids such as the derivatives of methane-1, 1-diphosphonic acid (Nash et al., 1995). The protonation of subsequent sites in multifunctional acids has a less consistent impact on protonation enthalpies, but for carboxylic acids, it generally leads to progressively less endothermic/more exothermic protonation enthalpies, as typified by citric or malonic acid.

Consequently, the thermodynamic parameters derived from our primary, 4-site, data analysis supports the previous assignments of Sites 1–3 from the 4-site model. In addition, these parameters also suggest that the functional groups on the bacterial surface behave more like multifunctional organic acids with nearby proton-active sites rather than simple monofunctional acids with a single isolated functional group. Thus, multifunctional organic acids are likely better analogues than monofunctional acids in modeling the acidity behavior of the functional groups present on bacterial surfaces. This perspective is also supported by the thermodynamic parameters for the protonation of the carboxylate sites of the highly multifunctional humic and fulvic acids. (Choppin and Kullberg, 1978; Perdue, 1978; Rao and Choppin, 1995). The protonation enthalpies for the more acidic sites of these polyfunctional molecules ($pK_a < 8$) are exothermic (−0.4 to −13.9 kJ/mol), just as we observe for the bacterial surface. Likewise the protonation entropies, +66 to +86 J/mol K, are somewhat smaller than the values found for the first protonation step of most carboxylic acids. In the absence of corroborating spectroscopic data, any comments about the identity Site 4 would be only speculative. The enthalpy of Site 4 is much more exothermic than would be expected for carboxylic or phosphonic acids and may be more consistent with amine or hydroxyl functional groups, such as phenols.

The thermodynamic parameters derived from our alternative data analysis involving the Langmuir–Freundlich 2-site protonation model also are consistent with this interpretation. That is, the thermodynamic parameters from the Langmuir–Freundlich treatment indicate that the functional groups on the bacterial surface behave more like multifunctional carboxylic or organo-phosphonic acids due to protonation enthalpies being exothermic (e.g., −3.6 kJ/mol for Site 1). This additional analysis illustrates that, despite the chosen model of the bacterial surface protonation, the bulk exothermic enthalpies and nature of proton binding put rigorous constraints on the site-specific enthalpies one can derive.

3.5. Cd adsorption reactions

The cumulative background corrected heat evolved by titration of a $Cd(ClO_4)_2$ solution into the bacterial suspension is shown as a function of the total moles of Cd added in Fig. 4. In contrast to the protonation experiments, where we observed exothermic heats, the bulk heats produced as Cd adsorbs onto the bacterial surface are endothermic, in general agreement with the observation of Weppen and Hornburg (1995). The continued uptake of heat at the highest Cd concentrations illustrates that the bacterial surface did not reach saturation and continued to adsorb Cd

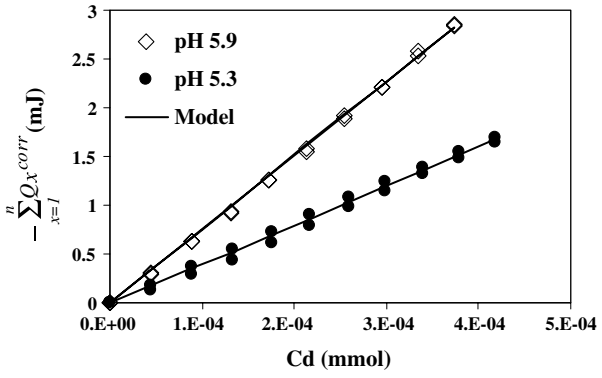

Fig. 4. Cumulative background corrected heat ($-\sum_{x=1}^{n} Q_x^{corr}$) generated by titration of 5.3 mM $Cd(ClO_4)_2$ into 80 g/L *B. subtilis* starting at pH 6.0 or 5.3, with the curve representing the fit to Eq. (7). Negative Q represents endothermic heats.

throughout the titration experiment. In fact, the maximum Cd loading never exceeded 15% of the proton capacity of even the lowest concentration site on the *B. subtilis* surface.

For the calorimetry measurements of surface protonation, the background corrected heat is only a product of proton adsorption reactions; however, for the Cd adsorption titrations, the background corrected heat includes the heat from both Cd-bacterial wall adsorption reactions and protonation/deprotonation reactions that occur as the bacterial suspension comes to equilibrium after each addition of Cd. In the pH ranges studied, the pH change caused by each Cd addition is small (the total pH change over an entire titration was $\leqslant 0.1$ in both cases), because the pH of the bacterial suspension and the titrant were well matched. Despite this, Cd adsorption alters the concentration of free adsorption sites, L_i^-, which causes the concentration of the HL_i sites to shift accordingly. In the Cd adsorption titrations, changes in the degree of protonation are responsible for ca. 30% of the background corrected heat and must be accounted for when calculating the enthalpies of Cd adsorption.

Eq. (7) describes the relationship between the cumulative background corrected heat at the xth addition of Cd, and the individual contributions from each adsorption site (omitting charges on the Cd species for simplicity)

$$-\sum_{x=1}^{n} Q_x^{\text{corr}} = \sum_{i=1}^{4} (\Delta H_{\text{CdL}_i} n^x_{\text{CdL}_i} + \Delta H_{\text{HL}_i} n^x_{\text{HL}_i}), \tag{7}$$

where ΔH_{CdL_i} is the enthalpy of adsorption of Cd onto site L_i^- per mole of CdL_i formed, $n^x_{\text{CdL}_i}$ represents the total number of moles of Cd adsorbed onto site L_i^-, and $n^x_{\text{HL}_i}$ represents the change in the number of moles of species HL_i from the beginning of the titration. Values for $n^x_{\text{CdL}_i}$ at each point of the titration are determined from the Cd adsorption model of Borrok et al. (2004b), who used bulk measurements of Cd adsorption onto *B. subtilis* to derive stability constants for the important Cd-bacterial surface complexes. Their model was based on the bacterial surface protonation model of Fein et al. (2005), and involved Cd adsorption onto bacterial surface Sites 2 and 3 with the following reaction stoichiometry:

$$L_i^- + Cd^{2+} \leftrightarrow CdL_i^-. \tag{8}$$

Alternate attempts to model Cd adsorption data using the Langmuir–Freundlich model for the bacterial surface protonation reactions could not successfully reproduce the extents of adsorption observed under the conditions of the calorimetric titrations; consequently, for the Cd data analysis we only considered the model by Borrok et al. (2004b). Using Fein's protonation constants, Borrok's stability constants (corrected to 0.1 M ionic strength using the Davies equation), and the known total concentrations of Cd, protons, and each of the L_i sites, one can calculate the values of $n^x_{\text{CdL}_i}$ and $n^x_{\text{HL}_i}$ associated with each addition of Cd-containing titrant during the experiment. Since $n^x_{\text{CdL}_1}$ and $n^x_{\text{CdL}_4}$ are zero in the Borrok model of Cd adsorption, Eq. (7) contains two unknown parameters, ΔH_{CdL_2} and ΔH_{CdL_3}. The best fit of these parameters to the Cd titrations at pH 5.34 and 5.95 gives enthalpies of -0.2 ± 0.4 and $+14.4 \pm 0.9$ kJ/mol for Cd adsorbing onto Sites 2 and 3, respectively (Fig. 4).

The Cd adsorption enthalpies derived from our calorimetric measurement are relatively insensitive to the uncertainties in the protonation enthalpies of Sites 1–3. Inaccuracies in the protonation enthalpy of Site 3 would have the largest impact on the derived Cd-binding enthalpies, but varying ΔH_{HL_3} within its 2σ uncertainty limits changes the Cd adsorption enthalpies by 0.3 kJ/mol, which is significantly less than the uncertainty in the fit. Using the same approach that we used to calculate the protonation entropies, we calculate the following entropies of Cd adsorption, $+57 \pm 4$ and $+128 \pm 5$ J/mol K, at Sites 2 and 3, respectively.

3.6. Implications of the derived enthalpies and entropies

The calculated values for the enthalpies of Cd adsorption by the bacterial surface are similar to those expected for Cd complexation by anionic oxygen ligands, which are typically endothermic to slightly exothermic (Martell et al., 1998). The similarity in enthalpies suggests that the binding mechanisms between metals and the anionic oxygens on organic acids such as citrate and acetate are similar to those that are responsible for Cd binding to the organic acid functional group sites on the bacterial surface. This explains the success of predictive tools such as the linear free energy correlations invoked by Fein et al. (2001), who demonstrated a relationship between measured stability constants for metal-bacterial surface complexes and corresponding metal-organic acid anion stability constants. Similarities in binding environments make these predictive tools possible and are likely the cause of the similar enthalpies of Cd adsorption onto the bacterial surface functional groups.

Entropies of complexation can provide information on the coordination environment of complexed metals, e.g., inner sphere versus outer sphere complexation and metal–ligand stoichiometries. The formation of a metal–ligand complex in solution would initially seem to decrease the number of particles in a solution, thus imparting order and causing a decrease in the entropy of the system ($\Delta S < 0$). This is often untrue. Inner sphere complexes have *positive* entropies of complexation because the complexation event displaces solvating water molecules from the coordination sites of the metal and ligand. The displacement of water molecules from the coordination sites increases the disorder of the system, causing large positive entropies of complexation (Nancollas, 1966). Negative complexation entropies, on the other hand, characterize outer sphere complexes because the formation of outer sphere complexes does not displace any coordinated water molecules when a metal ion associates with the ligand functional group. In addition to the lack of dehydration during

outer sphere complexation, the association of the metal and ligand decreases the number of particles in the solution, further increasing the order in the system and resulting in more negative entropies of complexation. The entropies of Cd complexation onto bacterial surface Sites 2 and 3 derived from our experiments are both significantly positive, which is indicative of inner sphere coordination. These results are fully consistent with EXAFS that found inner sphere binding of Cd onto carboxyl and phosphoryl groups on *B. subtilis* (Boyanov et al., 2003).

The magnitude of a complexation entropy is related to the extent of dehydration caused by complexation and consequently to the identity and number of ligands binding the metal (Choppin, 1997; Jensen et al., 2000). Therefore, the entropy of complexation can provide information not only on the nature of complexation, but also on the number of ligands involved in the complexation. Typical complexation entropies for inner sphere binding of Cd with a single deprotonated carboxyl ligand such as acetic, ethoxyacetic, or phenylthio acetic acid, range between +30 and +50 J/mol K (Martell et al., 1998), with an average of $+35 \pm 5$ J/mol K per carboxylate. This can be compared to the value reported for a more weakly hydrated divalent cation, Ca^{2+}, which is $+25 \pm 4$ J/mol K per bound carboxylate (Rizkalla and Choppin, 1992). Entropies for the inner sphere binding of Cd to deprotonated phosphoryl ligands ($R–PO_3^{2-}$) are expected to be approximately +65 J/mol K per bound phosphoryl, based on empirical ratios of the complexation entropies obtained for the 1:1 complexes of other divalent metal cations with related dicarboxylate and diphosphonate ligands (Martell et al., 1998). While these values are approximate, they can provide some constraints on Cd binding onto the bacterial cell wall. For example, since the binding of Cd to two spatially constrained phosphoryl groups will displace approximately twice the number of water molecules as binding to a single group, the entropies associated with Cd-bisphosphoryl binding should be twice that of Cd-phosphoryl binding, and would therefore likely be ca. +130 J/mol K.

Within this framework, the measured entropy of Cd adsorption onto bacterial surface Site 2 (+57 J/mol K), suggests that each Cd ion is bound to an average of one to two Site 2 ligands ($57/35 = 1.6$), if as suggested by EXAFS experiments, Site 2 is composed of carboxyl functionalities (Kelly et al., 2002; Boyanov et al., 2003). Our calculated entropy of Cd adsorption onto bacterial surface Site 3 (+128 J/mol K), which is most likely a phosphoryl functional group, would then suggest that Cd is bound to two ligands in Site 3 ($128/65 = 2.0$). These results are consistent with the EXAFS study of Boyanov et al. (2003), who examined Cd adsorption onto *B. subtilis* cells, and found evidence for inner sphere binding of Cd onto phosphoryl sites under pH conditions above 5.9. The entropies of Cd adsorption at Site 2 from our study provide additional constraints on the binding that occurs below pH 5.9, experimental conditions at which the stoichiometry of binding could not be resolved using EXAFS (Boyanov et al., 2003).

Estimations of the temperature dependence of proton adsorption based on the enthalpies suggest that little change in the acidity constants occurs with increasing temperature between 25 and 75 °C for Sites 1–3, and a modest change occurs for Site 4. These estimates for Sites 1–3 are consistent with the only experimental data available on protonation behavior of *B. subtilis* at elevated temperatures. Potentiometric titrations of *B. subtilis* at elevated temperatures have shown there to be little if any temperature dependence, up to a temperature of 75 °C, of the protonation constant for functional groups whose pK_a is below 7.7 (Wightman et al., 2001). If we assume that the ΔC_p values, the relative heat capacities of the products and the reactants, are zero for the protonation reactions, we can use the van't Hoff equation, in conjunction with the enthalpies from this study to calculate the expected temperature dependence of the protonation constants. The calculated acidity constants for the *B. subtilis* functional groups decrease approximately 0.1 log units between 25 and 75 °C for Sites 1 and 2, 0.4 log units for Site 3, and 0.9 log units for Site 4. The expected changes in acidity constants for Sites 1–3 are too small to be reliably quantified by acid—base titrations at elevated temperature. The expected change to the Site 4 acidity constant is more significant, but may also reflect the relatively higher uncertainties associated with the Site 4 enthalpy of protonation compared to the values for the other sites. The titrations in the Wightman et al. (2001) study did not exceed pH 9; therefore, their model of the bacterial surface did not include a fourth site with a pK_a above 7.7. Consequently, our expected change for the pK_a's of Sites 1–3 is within the reported error limits of the pK_a's associated with the 3-site model of Wightman et al. (2001). Performing similar calculations with the van't Hoff equation using our enthalpies of Cd adsorption and assuming $\Delta C_p = 0$ for the Cd adsorption reactions yields a predicted decrease in the log K value of Cd adsorbing onto Site 2 of 0.005 log units and an increase of 0.4 log units for Site 3 between 25 and 75 °C. This suggests that Cd adsorption onto Site 2 at elevated temperatures can be determined reasonably accurately using the stability constant for Cd adsorption reactions from 25 °C experiments. Our predicted stability constant for Cd adsorption onto Site 3 at 75 °C suggests that there would be a slight increase in Cd uptake, although the extent may not be detectable by bulk adsorption experiments.

4. Conclusions

Titration calorimetry of bacterial surface adsorption reactions is a powerful technique for gaining a new understanding of the reactivity of bacterial cell walls. Bulk calorimetry data are useful in gaining a qualitative view of the enthalpies and entropies, e.g., they differentiate between exothermic and endothermic reactions and provide constraints on bulk adsorption. The bulk heat measurements of bacterial surface protonation reactions in this study indicate that bacterial surface functional groups are not fully

protonated under the pH conditions studied, even at pH values as low as 2.5. Interpretation of the measured bulk heats in this study, using a surface complexation model of the bacterial surface to determine the relative contributions to the bulk heat from individual functional groups, yields site-specific enthalpies and entropies of protonation and Cd adsorption onto *B. subtilis*. These data provide mechanistic details of proton and Cd adsorption that are impossible to glean from bulk adsorption experiments, spectroscopic approaches, or from thermodynamic modeling alone. The molecular-scale information that calorimetry offers significantly enhances our understanding of bacterial cell wall reactivity, and improves our ability to incorporate bacterial adsorption reactions into geochemical models of mass transport in geologic systems.

Acknowledgments

Research funding was provided by the National Science Foundation through an Environmental Molecular Science Institute Grant (EAR02-21966). The work at Argonne National Laboratory, managed by the University of Chicago, was funded by the US Department of Energy, Office of Basic Energy Sciences—Chemical Sciences and the EMSI program under contract W-31-109-ENG-38. Journal reviews and the comments made by Associate Editor Michael Machesky were particularly helpful in improving the presentation of this work.

Associate editor: Michael L. Machesky

References

Borrok, D., Fein, J.B., Kulpa, C.F., 2004a. Proton and Cd adsorption onto natural bacterial consortia: testing universal adsorption behavior. *Geochim. Cosmochim. Acta* **68** (15), 3231–3238.

Borrok, D., Fein, J.B., Tischler, M., O'Loughlin, E., Meyer, H., Liss, M., Kemner, K.M., 2004b. The effect of acidic solutions and growth conditions on the adsorptive properties of bacterial surfaces. *Chem. Geol.* **209** (1–2), 107–119.

Boyanov, M.I., Kelly, S.D., Kemner, K.M., Bunker, B.A., Fein, J.B., Fowle, D.A., 2003. Adsorption of cadmium to *Bacillus subtilis* bacterial cell walls: a pH-dependent X-ray absorption fine structure spectroscopy study. *Geochim. Cosmochim. Acta* **67** (18), 3299–3311.

Chatellier, X., Fortin, D., 2004. Adsorption of ferrous ions onto *Bacillus subtilis* cells. *Chem. Geol.* **212** (3–4), 209–228.

Choppin, G.R., 1997. Factors in Ln(III) complexation. *J. Alloy. Compd.* **249** (1–2), 1–8.

Choppin, G.R., Kullberg, L., 1978. Protonation thermodynamics of humic acid. *J. Inorg. Nucl. Chem.* **40**, 651–654.

Christensen, J.J., Hansen, L.D., Izatt, R.M., 1976. *Handbook of Proton Ionization Heats and Related Thermodynamic Quantities*. Wiley-Interscience, New York.

Christensen, J.J., Izatt, R.M., Hansen, L.D., 1967. Thermodynamics of proton ionization in dilute aqueous solution. VII. ΔH and ΔS values for proton ionization from carboxylic acids at 25°. *J. Am. Chem. Soc.* **89**, 213–222.

Cox, J.S., Smith, D.S., Warren, L.A., Ferris, F.G., 1999. Characterizing heterogeneous bacterial surface functional groups using discrete affinity spectra for proton binding. *Environ. Sci. Technol.* **33** (24), 4514–4521.

Daughney, C.J., Fein, J.B., 1998. Sorption of 2,4,6-trichlorophenol by *Bacillus subtilis*. *Environ. Sci. Technol.* **32** (6), 749–752.

Daughney, C.J., Siciliano, S.D., Rencz, A.N., Lean, D., Fortin, D., 2002. Hg(II) adsorption by bacteria: a surface complexation model and its application to shallow acidic lakes and wetlands in Kejimkujik National Park, Nova Scotia, Canada. *Environ. Sci. Technol.* **36** (7), 1546–1553.

Fein, J.B., Boily, J.-F., Yee, N., Gorman-Lewis, D., Turner, B.F., 2005. Potentiometric titrations of *Bacillus subtilis* cells to low pH and a comparison of modeling approaches. *Geochim. Cosmochim. Acta* **69** (5), 1123–1132.

Fein, J.B., Daughney, C.J., Yee, N., Davis, T.A., 1997. A chemical equilibrium model for metal adsorption onto bacterial surfaces. *Geochim. Cosmochim. Acta* **61** (16), 3319–3328.

Fein, J.B., Martin, A.M., Wightman, P.G., 2001. Metal adsorption onto bacterial surfaces: development of a predictive approach. *Geochim. Cosmochim. Acta* **65** (23), 4267–4273.

Fowle, D.A., Fein, J.B., 1999. Competitive adsorption of metal cations onto two gram positive bacteria: testing the chemical equilibrium model. *Geochim. Cosmochim. Acta* **63** (19/20), 3059–3067.

Fowle, D.A., Fein, J.B., Martin, A.M., 2000. Experimental study of uranyl adsorption onto *Bacillus subtilis*. *Environ. Sci. Technol.* **34** (17), 3737–3741.

Gorman-Lewis, D., Fein, J.B., Soderholm, L., Jensen, M.P., Chiang, M.H., 2005. Experimental study of neptunyl adsorption onto Bacillus subtilis. *Geochim. Cosmochim. Acta* **69** (20), 4837–4844.

Grenthe, I., Ots, H., Ginstrup, O., 1970. A calorimetric determination of the enthalpy of ionization of water and the enthalpy of protonation of THAM at 5, 20, 25, 35, and 50 °C. *Acta Chem. Scand.* **24**, 1067–1080.

Haas, J.R., Dichristina, T.J., Wade, R., 2001. Thermodynamics of U(VI) sorption onto *Shewanella putrefaciens*. *Chem. Geol.* **180** (1–4), 33–54.

Hale, J.D., Izatt, R.M., Christensen, J.J., 1963. A calorimetric study of the heat of ionization of water at 25°. *J. Phys. Chem.* **67**, 2605–2608.

Hennig, C., Panak, P.J., Reich, T., Rossberg, A., Raff, J., Selenska-Pobell, S., Matz, W., Bucher, J.J., Bernhard, G., Nitsche, H., 2001. EXAFS investigation of uranium(VI) complexes formed at *Bacillus cereus* and *Bacillus sphaericus* surfaces. *Radiochim. Acta* **89** (10), 625–631.

Herbelin, A., Westall, J.C., 1994. FITEQL 3.1, A computer program for determination of chemical equilibrium constants from experimental data. *Dept. Chem. Oregon State Univ.*.

Jensen, M.P., Morss, L.R., Beitz, J.V., Ensor, D.D., 2000. Aqueous complexation of trivalent lanthanide and actinide cations by *N*,*N*,*N*′,*N*′-Tetrakis(2-pyridylmethyl)ethylenediamine. *J. Alloy. Compd.* **303/304**, 137–141.

Jespersen, N.D., Jordan, J., 1970. Thermometric enthalpy titration of proteins. *Anal. Lett.* **3**, 323–334.

Kelly, S.D., Kemner, K.M., Fein, J.B., Fowle, D.A., Boyanov, M.I., Bunker, B.A., Yee, N., 2002. X-ray absorption fine structure determination of pH-dependent U-bacterial cell wall interactions. *Geochim. Cosmochim. Acta* **66** (22), 3855–3871.

King, E.J., 1965. *Acid-Base Equilibria*. Macmillan, New York.

Koopal, L.K., Vanriemsdijk, W.H., Dewit, J.C.M., Benedetti, M.F., 1994. Analytical isotherm equations for multicomponent adsorption to heterogeneous surfaces. *J Colloid Interface Sci.* **166** (1), 51–60.

Lee, J.U., Fein, J.B., 2000. Experimental study of the effects of *Bacillus subtilis* on gibbsite dissolution rates under near-neutral pH and nutrient-poor conditions. *Chem. Geol.* **166** (3–4), 193–202.

Martell, A.E., Smith, R.M., Motekaitis, R.J., 1998. Critically Selected Stability Constants of Metal Complexes Database Version 5.0. In *NIST Standard Reference Database*, **vol. 46**. NIST Standard Reference Data.

Martinez, R.E., Smith, D.S., Kulczycki, E., Ferris, F.G., 2002. Determination of intrinsic bacterial surface acidity constants using a Donnan shell model and a continuous pK_a distribution method. *J. Colloid Interface Sci.* **253** (1), 130–139.

Nancollas, G.H., 1966. *Interactions in Electrolyte Solutions*. Elsevier, Amsterdam.

Nash, K.L., Rao, L.F., Choppin, G.R., 1995. Calorimetric and laser induced fluorescence investigation of the complexation geometry of selected europium-gem-diphosphonate complexes in acidic solutions. *Inorg. Chem.* **34**, 2753–2758.

Ngwenya, B.T., Sutherland, I.W., Kennedy, L., 2003. Comparison of the acid-base behaviour and metal adsorption characteristics of a gram-negative bacterium with other strains. *Appl. Geochem.* **18** (4), 527–538.

Panak, P.J., Knopp, R., Booth, C.H., Nitsche, H., 2002. Spectroscopic studies on the interaction of U(VI) with *Bacillus sphaericus*. *Radiochim. Acta* **90** (9–11), 779–783.

Perdue, E.M., 1978. Solution thermochemistry of humic substances-I. Acid-base equilibria of humic acid. *Geochim. Cosmochim. Acta* **42**, 1351–1358.

Plette, A.C.C., van Riemsdijk, W.H., Benedetti, M.F., Van der Wal, A., 1995. pH dependent charging behavior of isolated cell walls of a Gram-positive soil bacterium. *J. Colloid Interface Sci.* **173** (2), 354–363.

Rao, L., Choppin, G.R., 1995. Thermodynamic study of the complexation of neptunium(V) with humic acids. *Radiochim. Acta* **69**, 87–95.

Rizkalla, E.N., Choppin, G.R., 1992. Hydration of lanthanides and actinides in solution. *J. Alloy. Compd.* **180**, 325–336.

Sokolov, I., Smith, D.S., Henderson, G.S., Gorby, Y.A., Ferris, F.G., 2001. Cell surface electrochemical heterogeneity of the Fe(III)-reducing bacterium *Shewanella putrefaciens*. *Environ. Sci. Technol.* **35** (2), 341–347.

Vanderzee, C.E., Swanson, J.A., 1963. The heat of ionization of water. *J. Phys. Chem.* **67**, 2608–2612.

Weppen, P., Hornburg, A., 1995. Calorimetric studies on interactions of divalent cations and microorganisms or microbial envelopes. *Thermochim. Acta* **269/270**, 393–404.

Wightman, P.G., Fein, J.B., Wesolowski, D.J., Phelps, T.J., Benezeth, P., Palmer, D.A., 2001. Measurement of bacterial surface protonation constants for two species at elevated temperatures. *Geochim. Cosmochim. Acta* **65** (21), 3657–3669.

Yee, N., Fein, J., 2001. Cd adsorption onto bacterial surfaces: a universal adsorption edge? *Geochim. Cosmochim. Acta* **65** (13), 2037–2042.

Yee, N., Fowle, D.A., Ferris, F.G., 2004. A Donnan potential model for metal sorption onto *Bacillus subtilis*. *Geochim. Cosmochim. Acta* **68** (18), 3657–3664.

Zekany, L., Nagypal, I., 1985. A Comprehensive Program for the Evaluation of Potentiometric and/or Spectrophotometric Equilibrium Data Using Analytical Derivatives. In: *Computational Methods for the Determination of Formation Constants*. Plenum Press.